A Wideband Terahertz High-T_c Superconducting Josephson-Junction Mixer: Electromagnetic Design, Analysis and Characterization

Xiang Gao[1], Ting Zhang[1, 2], Jia Du[1], Andrew R. Weily[3], Yingjie Jay Guo[2], Cathy P. Foley[1]

[1] CSIRO Manufacturing, PO Box 218, Lindfield, NSW 2070, Australia;

[2] Global Big Data Technologies Centre, University of Technology Sydney, Ultimo, NSW 2007, Australia;

[3] CSIRO Data61, Marsfield, NSW 1710, Australia

Abstract

This paper presents a wideband terahertz (THz) mixer based on a thin-film antenna-coupled high-temperature superconducting (HTS) $YBa_2Cu_3O_{7-x}$ (YBCO) step-edge Josephson junction. The HTS mixer enables the flexible harmonic mixing operation at multiple THz bands with one same microwave local oscillator (LO) source, and features very wide intermediate-frequency (IF) or instantaneous bandwidth. In order to optimize the frequency down-conversion performance of the mixer, systematic electromagnetic design and analysis have been carried out to improve the power coupling of THz radiation as well as wideband transmission of microwave signals. Experimental characterization of a fabricated device prototype has demonstrated that the mixer exhibits good performance at both the 200 GHz and 600 GHz bands. Detailed measurement results including the DC characteristics, LO pumping requirement, frequency response, mixing linearity and conversion gain are presented in this paper.

1. Introduction

Over the last few years, there is a drastically increasing demand for high speed wireless transmission in various electronics application scenarios, such as short-range intra-machine and inter-board communications, medium-range wireless local and personal area networks, and long-range high-throughput wireless directional links. Benefitting from the considerable absolute bandwidth, terahertz (THz) wireless communication [1, 2] is envisioned as a promising technology to effectively alleviate the spectrum scarcity and capacity limitations of current wireless systems. However, there

also exists a significant challenge for THz communication, i.e., the very high path loss resulting from strong atmospheric absorption by water vapor, which poses a major constraint on the communication distance.

In order to overcome the atmospheric attenuation problem and exploit the great potential of THz communication, ultrasensitive heterodyne receivers are required for the detection of incoming weak THz signals. The performance of a heterodyne receiver critically depends on its frontend component, i.e. the frequency down-converter or mixer. High-temperature superconducting (HTS) Josephson-junctions are very attractive frequency down-converters for THz communication receivers due to their superior sensitivity, large bandwidth, and low local oscillator (LO) power requirement. Currently, the most sensitive THz mixers were achieved in low-T_c superconducting (LTS) devices [3-8]. These devices, however, operate at liquid helium temperature (4.2 K) or below and, due to the high cost associated with cryogenic instruments, they are mainly for high-end applications such as astronomical observation. The HTS devices, on the other hand, can operate at higher temperatures, where much cheaper cryogenic fluid (liquid nitrogen – 77 K) or cheaper and smaller single-stage commercial cryocoolers can be used for cooling the devices, thus offer the potentials in other applications like sensing and communication in THz bands.

Compared with the LTS counterpart, research progress on THz HTS mixer lags significantly behind because of the challenging junction technology. There are some early stage studies of THz HTS Josephson-junction mixers that have been reported in the open literature [9-14]. However, the results were mostly achieved in very low temperature ranges, where expensive and bulky cryogenic facilities were still required. Although HTS Josephson-junction mixing at higher temperatures has been observed at millimetre-wave band [15, 16], there are rarely any reports showing THz HTS mixers working at 40 to 77 K where a single-stage cryocooler can be used. In addition, the electromagnetic design and analysis were hardly discussed for these reported HTS mixer devices, which are extremely important for the improvement of signal coupling and isolation.

With the advanced HTS step-edge Josephson-junction technology, our group has in recent years developed a number of microwave HTS mixers [17-19] and THz HTS detectors [20, 21]. Very recently, we reported our first demonstration of a narrow-band THz HTS mixer operating at around 600 GHz [22]. In this paper, we present our new research results on developing a wideband THz HTS Josephson-junction frequency down-converter. The main new contributions in this work can be summarized below. (1) The presented mixer device features new promising functions, which not only enables the flexible operation at multiple different THz bands with one same microwave LO source, but also exhibits very wide intermediate-frequency (IF) or instantaneous bandwidth. Hence,

it is most suited for high data rate wireless communication as well as high-resolution remote sensing applications. (2) A systematic electromagnetic design was provided for improving the THz coupling and microwave signal transmission of the mixer module. There are a number of novel technical aspects proposed in this work, such as the impedance-based tuning technique to maximize the antenna coupling efficiency at the bands of interest, the analysis of the influence of the metal housing cover on radiation pattern, the inductive loading utilized in coplanar waveguide (CPW) line for parasitic capacitance compensation, and a novel packaging approach for avoiding unwanted resonances. (3) Detailed experimental characterizations were conducted for a fabricated mixer prototype at both 200 GHz and 600 GHz bands, and the measured results were comparatively presented for those two different THz bands. The mixer device has demonstrated superior performance than other HTS Josephson junction mixers reported to date, especially for its wide instantaneous bandwidth and the flexibility of multiple THz-band operation using one low-cost microwave LO source.

2. Electromagnetic Design and Analysis

2.1 THz Antenna Design

Quasi-optical coupling offers the advantages of reliable and low-cost fabrication as well as the convenience of integration with the HTS Josephson junction. Figure 1 shows the geometry of a THz log-periodic circular-toothed thin-film antenna. Based on this antenna, the incident THz wave can be effectively coupled into a Josephson junction located at the antenna port. Although the CPW transmission line and surrounding ground plane are present in the simulation model, the main radiator is the central log-periodic circular-toothed structure on an MgO substrate (relative permittivity: 9.63) and a high-resistivity silicon (Si) hemispherical lens (relative permittivity: 11.7) attached on the back of the MgO substrate for high radiation directivity in the negative Z direction.

The input impedance of THz log-periodic circular-toothed thin-film antenna, calculated using the software Computer Simulation Technology (CST) Microwave Studio, is shown in figure 2. It can be clearly seen that the input resistance and reactance traces display obvious log-periodic fluctuation characteristics as the operating frequency varies, with an average impedance of around 75-80 Ω, a typical value for a self-complementary antenna structure [23] on an MgO substrate. Also, the input resistance trace achieves either its maxima or minima when the input reactance passes through zero. Taking advantage of these characteristics, the antenna has been carefully designed through parametric optimizations especially for the farthest arm's outer radius R_1 and the log-periodic scaling

factor τ (equal to r_1^2 / R_1^2), so as to make its input resistance achieve the minimum values at around 200 GHz and 600 GHz, which helps reduce the mismatch between the THz antenna and Josephson Junction (normal resistance: around 5 Ω) at frequencies of interest. Figure 2 also shows the simulated coupling efficiency η_c of the THz antenna, which is defined as

$$\eta_c = \left(1 - |S_{11}|^2\right)\eta \tag{1}$$

where S_{11} is the reflection coefficient, and η is the radiation efficiency. It is clearly shown that the coupling efficiency is around -8 dB at 200 GHz and 600 GHz.

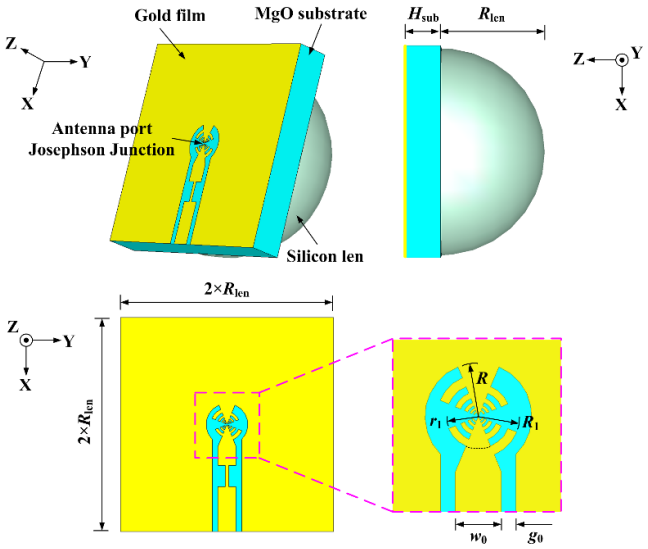

Figure 1. Geometry of a THz log-periodic circular-toothed thin-film antenna (H_{sub} = 0.5 mm, R_{len} = 1.5 mm, R = 293.90 μm, R_1 = 227.66 μm, r_1 = 176.34 μm, w_0 = 254 μm, g_0 = 80 μm, and log-periodic scaling factor τ = 0.6).

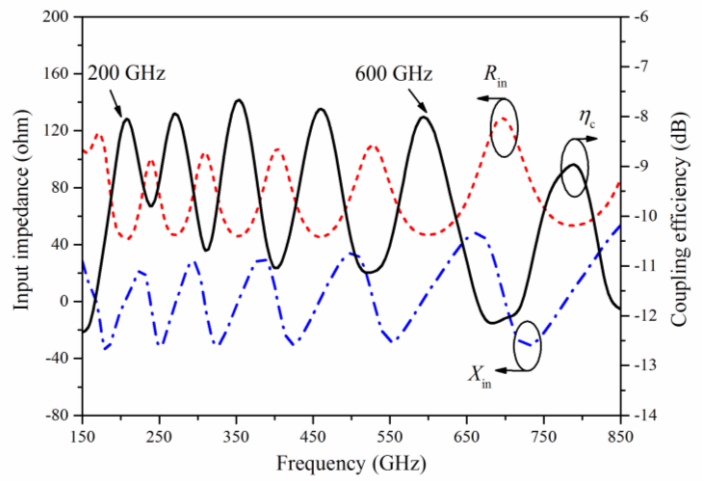

Figure 2. Simulated input impedance and coupling efficiency of a THz log-periodic circular-toothed thin-film antenna. (Red: input resistance R_{in}; blue: input reactance X_{in}; black: coupling efficiency η_c.)

Figure 3 shows the simulated radiation patterns of the THz antenna in the XZ and YZ planes at frequencies of 200 GHz and 600 GHz. It can be clearly seen that the radiation patterns exhibit high directivity along the negative Z direction, and the main beam becomes narrower as the operating frequency rises (half-power beam widths: 27° at 200 GHz and 10° at 600 GHz), which is expected due to the fixed aperture size of the Si lens. In addition, considering the THz antenna is to be mounted in a housing, it is necessary to investigate the effect of the housing's metal cover on the radiation patterns. The cover is a crucial element not only protecting the mixer chip from exposure but providing a good thermal contact of the mixer module with the coldhead in cryocooler. As shown in figure 3, the original small radiation back-lobe disappears due to the reflection of a metal housing cover placed at a height of Z = +2 mm from the thin-film antenna plane. However, the presence of a metal cover does not change the main-lobe but produces some extremely minor side-lobes. This is mainly benefited from the relatively high front-to-back ratio of the designed THz antenna.

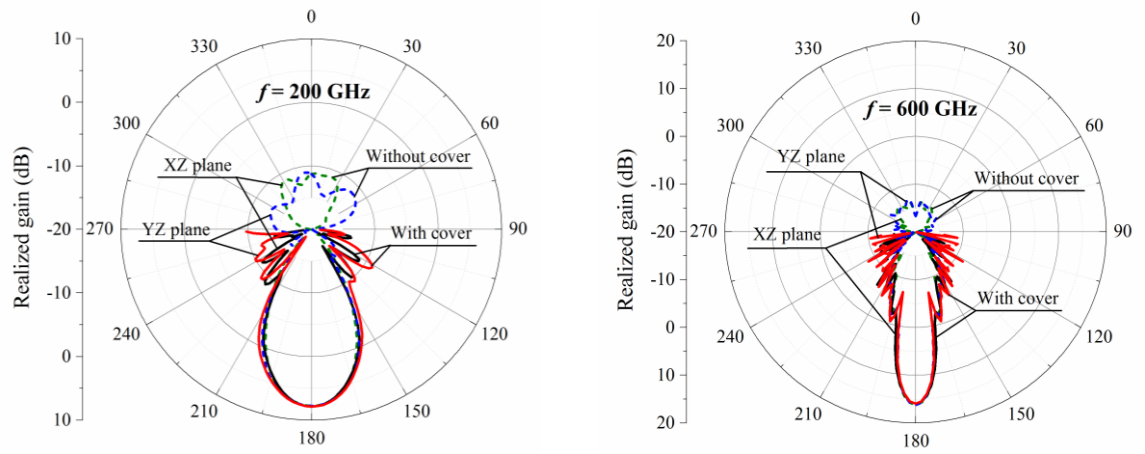

(a) (b)

Figure 3. Simulated radiation patterns of a THz log-periodic circular-toothed thin-film antenna at (a) 200 GHz and (b) 600 GHz. (Black: XZ plane, with cover; red: YZ plane, with cover; green: XZ plane, without cover; blue: YZ plane, without cover.)

Lastly, one point should be addressed based on simulation analysis. The surrounding CPW line and ground plane cause very little effects on the radiation performance of THz log-periodic thin-film antenna. This can be explained by observing the surface electric current distribution on the antenna structure, as shown in figure 4. Considering the radiation mechanism of the log-periodic antenna, the surface electric current only concentrates inside the active region whose location relies on the

operating frequency, and becomes extremely weak at the ends of two fan arms. Hence, there are almost no currents flowing onto the surrounding CPW line and ground plane. This analysis shows that the antenna design has the further advantage of not requiring a choke filter or isolation network to prevent the leakage of THz electric current.

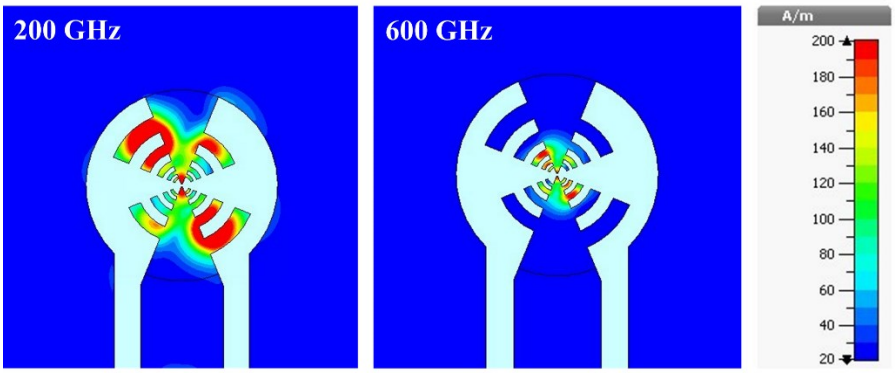

Figure 4. Simulated surface electric current distribution on a THz log-periodic circular-toothed thin-film antenna at 200 GHz and 600 GHz.

2.2 Microwave Coupling Design

Apart from the quasi-optical coupling of THz radiation, it is also extremely important to investigate the transmission characteristics of the microwave IF output signal. Figure 5 shows the simulation model of a microwave matching circuit, where two ports are defined at the position of the Josephson junction and the end of the CPW transmission line, respectively. The substrate (not shown in the model) is an MgO chip with thickness of 0.5 mm, and the Si lens is located on the back of the substrate. Considering the dynamic resistance of the Josephson junction varies (usually in an order of tens of Ω) depending on the junction parameters (critical current I_c and normal resistance R_n) and operating temperature, the two port impedances are set as 50 Ω and a 50-Ω CPW microwave transmission line is designed for matching. However, the discontinuity near the Josephson junction creates an additional capacitive reactance which deteriorates the impedance matching at higher frequencies. In order to overcome this matching problem, a short high-impedance transmission line element is placed at an appropriate position on the CPW line to behave as a lumped inductor to compensate for the parasitic capacitance.

Figure 6 shows the simulated reflection and transmission coefficients of the microwave matching circuit. It can be clearly seen that the impedance matching deteriorates at operating frequencies

above 25 GHz, provided there is no inductive compensation introduced. In comparison, after the loading of a short high-impedance transmission line element, the matching is significantly improved and remains very good until 40 GHz. Here, the size and position parameters of the inductive line has been optimized by using High Frequency Structural Simulator (HFSS) software.

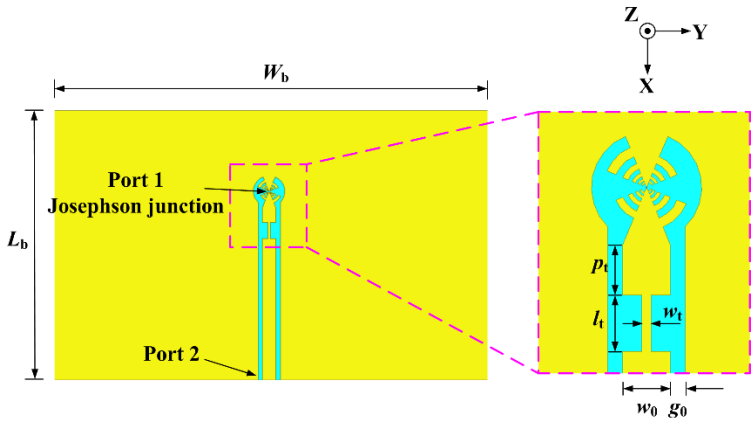

Figure 5. Simulated model of a microwave matching circuit (L_b = 5 mm, W_b = 10 mm, p_t = 264.93 μm, l_t = 300 μm, w_t = 50 μm, w_0 = 254 μm, g_0 = 80 μm).

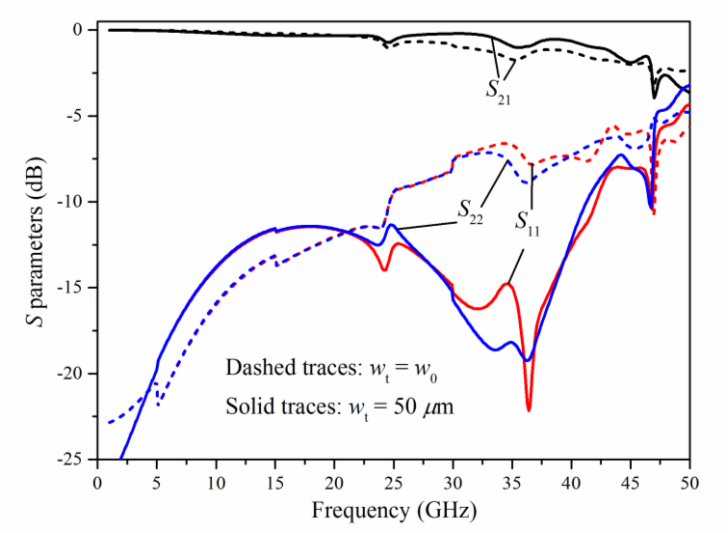

Figure 6. Simulated reflection and transmission coefficients of a microwave matching circuit without (dashed traces) and with (solid traces) inductive loading. (Red: S_{11}; blue: S_{22}; black: S_{21}.)

2.3 Chip Packaging Design

It is necessary to further examine the transmission performance of the microwave matching circuit while the mixer chip is mounted into a metal housing. As shown in figure 7(a), the conventional packaging approach is to locate the MgO chip on the housing base which contains a window for

placing the Si lens. Figure 8 shows the simulated reflection and transmission coefficients for this mounting method, from which it is clearly seen that a lot of detrimental spikes appear in the traces. This phenomenon can be explained as follows. For the mounting method shown in figure 7(a), the original ungrounded CPW line has become grounded due to the presence of the metal housing base. However, since there are no conducting via-holes connecting the top and bottom ground planes, the parasitic parallel-plate modes of grounded CPW line can be easily excited, which propagate and cause undesirable resonances.

Unfortunately, fabricating the conducting via-holes through the brittle MgO substrate along the CPW transmission line risks damaging the device chip, so is not a practical solution. In order to overcome the undesired resonance problem, an improved packaging method was proposed as shown in figure 7(b). Here, the MgO chip is placed in such a way that its top side thin-film Au ground plane is pressed against the housing plates using silver epoxy as the conductive adhesive. As clearly shown in figure 8, the microwave reflection and transmission characteristics for this new packaging approach has greatly improved compared with that of the conventional one; the unwanted resonant spikes have been removed.

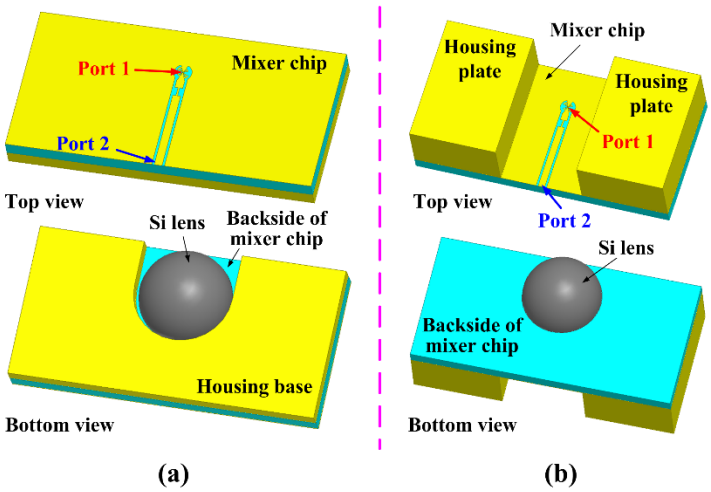

Figure 7. Simulated models: (a) conventional packaging: mixer chip on housing base; (b) improved packaging: mixer chip located below and against housing plates.

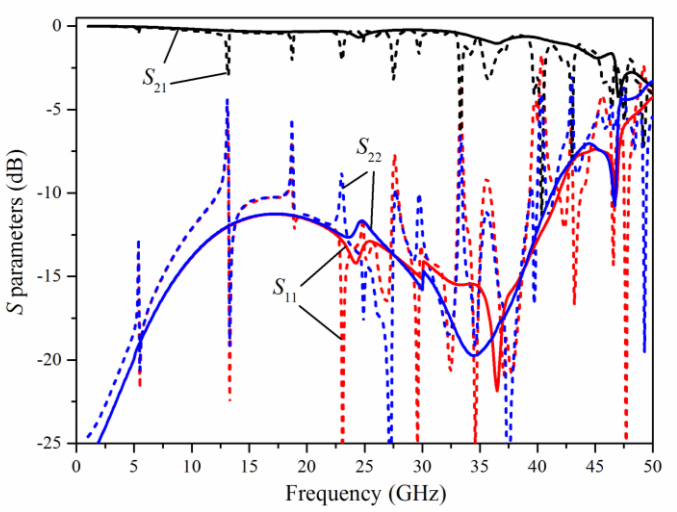

Figure 8. Simulated reflection and transmission coefficients for conventional (dashed traces) and improved (solid traces) packaging approaches. (red: S_{11}; blue: S_{22}; black: S_{21}.)

3. Experimental Details

Based on the systematic electromagnetic design and analysis, a wideband THz HTS Josephson-junction mixer module was fabricated and the photographs of the packaged module and patterned device are shown in figure 9. The MgO mixer chip is packaged using the proposed approach in figure 7(b), and then secured with two small thin-plates on its backside. Here, two mixer devices were fabricated on a 10×10-mm^2 MgO substrate, and two 3 mm diameter Si hemispherical lens were mounted on the back of the substrate and side by side as shown in the bottom view. In addition, two 5×10-mm^2 Bias-Tee printed circuit boards (PCBs) are located adjacently to both sides of the MgO chip, respectively. The in-house designed Bias-Tee network was implemented on a 0.254-mm thick polished Alumina substrate, which could operate up to 40 GHz and provides good isolation between the DC and microwave signals. Some resistors and capacitors are utilized in the DC biasing lines for electrostatic protection and interference prevention. The HTS mixer chip was fabricated at our laboratory using the well-established step-edge $YBa_2Cu_3O_{7-x}$ (YBCO) junction technology [24]. Briefly, after the step-edge patterns were created on the MgO substrate using a standard photolithography and Ar-ion beam milling, a ~200 nm thick YBCO film with a 50 nm in-situ Au film on top was deposited on the MgO substrate by Ceraco GmbH. The YBCO film has a smooth surface morphology with a film critical current density J_c of 2.4 MA/cm^2 and a critical temperature T_c of 86.2 K. The YBCO film was then patterned and etched to form the step-edge junctions and DC bias lines, and the in-situ Au was removed from the junction area. An additional layer of ~300 nm Au thin film was

subsequently deposited and patterned to form the Au thin-film antenna. The micrograph of the THz thin-film antenna and Josephson junction are shown in the inset of figure 9, where the YBCO step-edge junction is located between the two wings of the Au thin-film log-periodic antenna.

The THz HTS Josephson-junction mixer was measured using the harmonic mixing operation, which offers the advantage of removing the requirement of a second THz source and thus reducing the cost and complexity of system. Figure 10 shows the schematic diagram of the harmonic-mixing measurement set-up. The THz sources we used are two commercial solid-state Active Multiplier Chains (AMC) from Millitech and VDI, which can generate continuous wave radiation at 200 GHz and 600 GHz bands respectively when driven by an Agilent E8257D microwave generator. The radiation beam from the THz source is collimated and then focused onto the Si lens of the THz mixer module mounted inside a cryocooler. The THz signal is mixed with the high-order harmonic of a LO pumping signal generated by a Wiltron 68075B microwave generator. The LO signal shares the same port on the mixer module with the down-converted IF signal through a diplexer mounted outside of the cryocooler. The IF signal is then amplified by an IF low noise amplifier (MITEQ AFS3-00100600-20-ULN with a gain of 30 dB and noise figure of 2 dB) at room temperature. A battery-operated DC current source and an Agilent E4407B spectrum analyzer were utilized for DC biasing and recording IF output, respectively. In addition, two wire-grid polarizers (one rotatable and the other fixed) were added in the quasi-optics link to adjust the THz power for linearity measurement. They were placed in 45° tilted orientations for preventing multiple reflections between them.

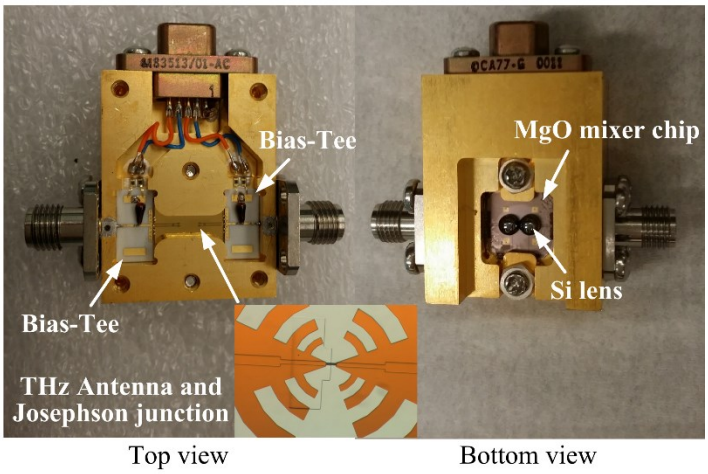

Figure 9. Photographs of a packaged wideband THz HTS Josephson-junction mixer module. Inset is a micrograph showing the enlarged view of a THz log-periodic thin-film antenna and step-edge Josephson junction.

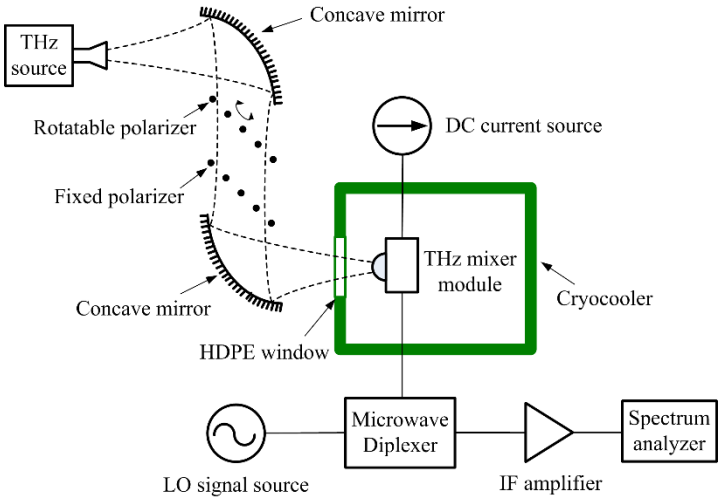

Figure 10. The schematic diagram of harmonic-mixing measurement set-up for the wideband THz HTS Josephson-junction mixer.

4. Mixer Characterizations

The step-edge junction displays a well-defined resistively-shunted-junction (RSJ) behavior in all measured temperatures between 20 to 77 K, with a normal resistance $R_n \approx 5\ \Omega$ and a junction critical current I_c between 15 μA (77 K) and 500 μA (20 K). The correspondent junction characteristic voltage $V_c = I_c R_n$ increases from 75 μV at 77 K to 2.5 mV at 20 K, corresponding to a characteristic frequency f_c of 36 GHz to 1.2 THz. The junction characteristics are well suited for the active device application from microwave to THz frequency ranges.

The HTS Josephson-junction mixer has been characterized at temperatures between 40 K and 77 K, a range that is attainable with a single-stage portable cryocooler. The mixer was found to operate stably at all measured temperatures, although the output signal-to-noise ratio (SNR) decreases with increasing working temperature due to the smaller conversion gain and higher mixer noise at higher temperatures. The fact that our mixer could operate at 77 K is a striking result as, to the best of our knowledge, the reported THz HTS mixers in literature to date (except for our very recent reported narrow-band THz mixer [22]) all operated in the temperatures lower than 77 K. For clarity, only exemplar results at 40 K are presented in this paper.

Figure 11 shows the measured DC current-voltage characteristics (IVCs) of the HTS Josephson-junction mixer under illumination of the ~200 and ~600 GHz radiation. It can be clearly seen that, the unpumped junction exhibits a critical current $I_c \approx 320$ μA at temperature of 40 K. Under the THz

illumination, the I_c of Josephson junction is partly suppressed and Shapiro steps appears in the traces. As predicted by the Josephson voltage-frequency equation [25]: $f = (2e/h) \times V = 0.4836 \times V$ (GHz) (V is the DC voltage in μV), the Shapiro voltage steps correspond to 194.4 GHz (red trace) and 602.4 GHz (blue trace) respectively. The results have demonstrated that the THz radiation is effectively coupled into the Josephson junction via the lens and antenna at both 200 GHz and 600 GHz bands.

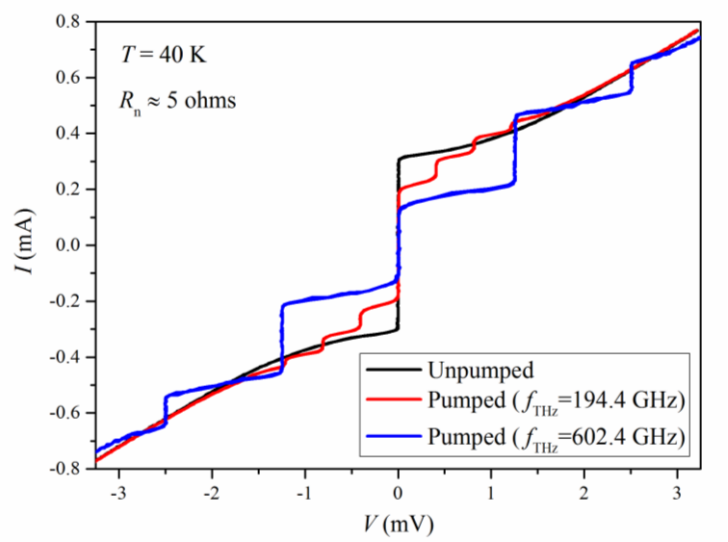

Figure 11. DC IVCs of the wideband THz HTS Josephson-junction mixer.

Figure 12(a) and 12(b) show the measured relationship of IF output power P_{IF} with LO pumping power P_{LO} at bath temperature of 40 K for the 200 GHz and 600 GHz bands, respectively. The bias current I_B was above the pumped junction critical current I_C and adjusted to yield maximum IF output. For harmonic mixer, the frequency relationship between the IF, THz and LO signals is: $f_{IF} = |f_{THz} - nf_{LO}|$ (where n is the harmonic order). Under a similar LO signal frequency of ~30 GHz, the harmonic mixing orders are 6th and 20th for 200 GHz and 600 GHz bands respectively. It can be seen that the P_{IF} rises with the increase of P_{LO} initially and then tends to plateau. The plateau appears at $P_{LO} \approx$ -36 dBm for the 6th harmonic mixing at 200 GHz and $P_{LO} \approx$ -31 dBm for the 20th harmonic mixing at 600 GHz band. Hence, the required LO power for normal operation at both bands is only in the order of μW, much lower than that required for pumping a semiconductor mixer, which is one of the major advantages of the Josephson-junction mixer.

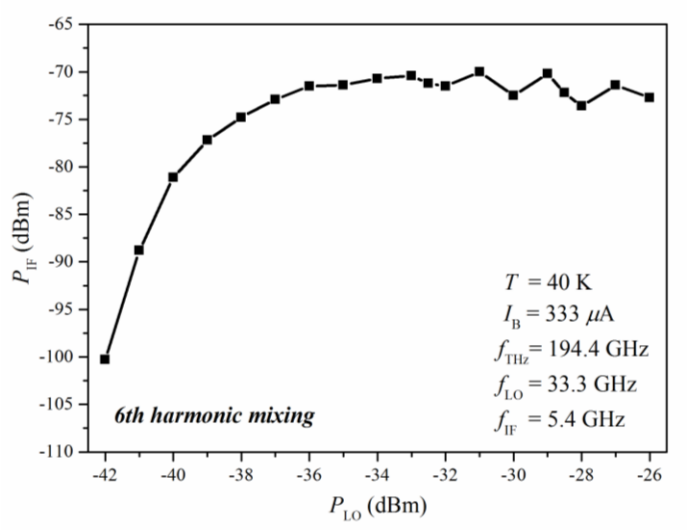

(a)

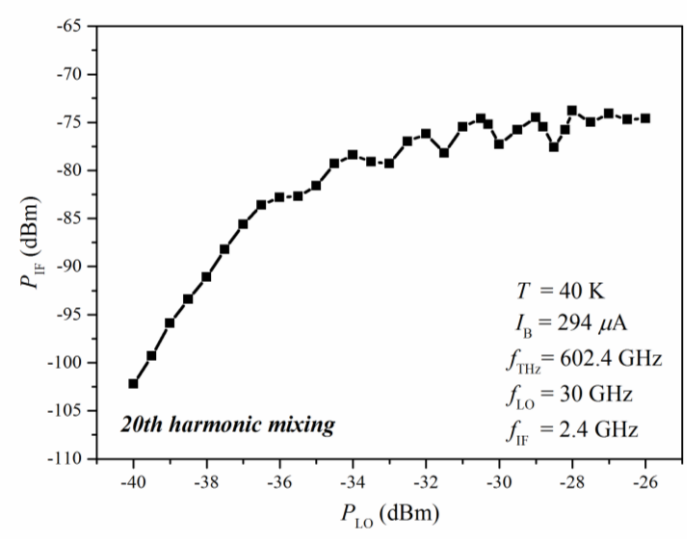

(b)

Figure 12. IF output power P_{IF} versus LO pumping power P_{LO} at (a) 200 GHz and (b) 600 GHz bands.

Figure 13 shows the measured frequency response of the THz HTS Josephson-junction mixer at both 200 GHz and 600 GHz bands. Based on the 6th and 20th harmonic mixing characterizations at respective bands, the directly measured IF bandwidth is around 8 GHz for either upper or lower sidebands. This bandwidth restriction is mainly due to the IF amplifier used. After a calibration of the whole IF link including cables, diplexer and IF amplifier as well as the THz source power variation with regard to operating frequency, it is found that the THz HTS mixer exhibits a wide IF bandwidth of at least 12 GHz for either upper or lower sidebands thus achieving an instantaneous bandwidth of 24 GHz for double sideband (DSB) applications. The small fluctuation in the frequency response

traces are due to the imperfect quasi-optics link as well as measurement and calibration tolerances. The steep drop at the band centre is in good agreement with the DC and low-frequency isolation characteristics of Bias-Tee network. It should be emphasized so far, this is the first time that a wide IF or instantaneous bandwidth has been achieved and reported for THz HTS mixer.

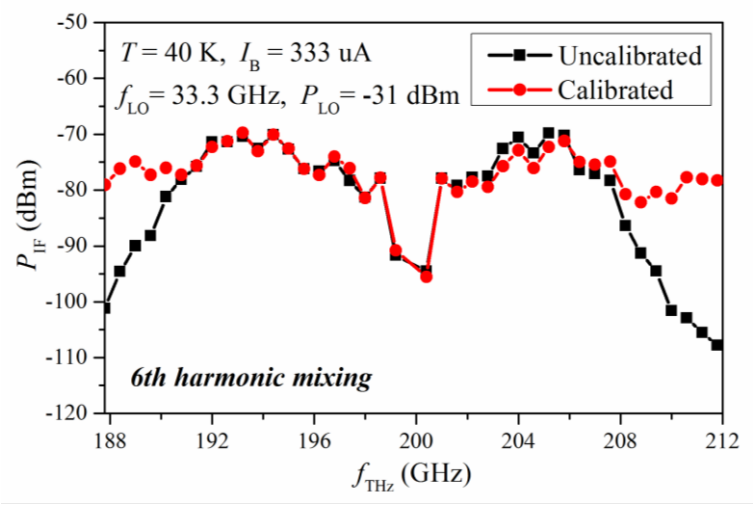

(a)

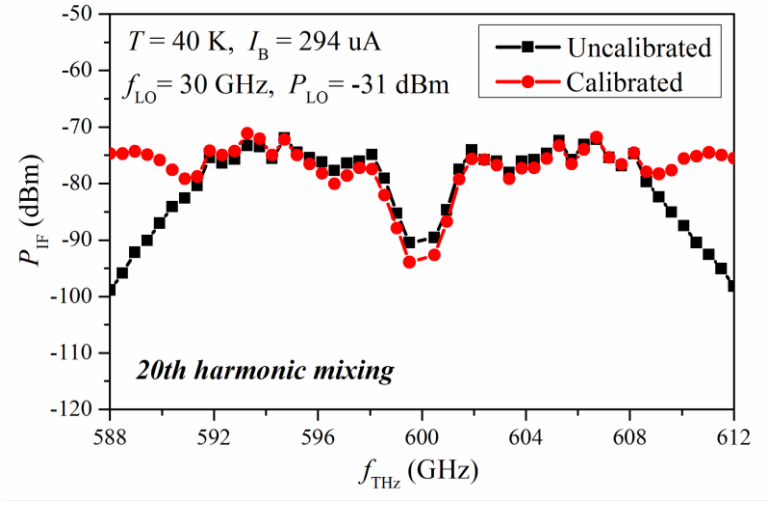

(b)

Figure 13. Frequency response of the wideband THz HTS Josephson-junction mixer at (a) 200 GHz and (b) 600 GHz bands.

Figure 14 shows the measured linearity and conversion gain of the THz HTS Josephson-junction mixer at temperature of 40 K for 200 GHz and 600 GHz bands. As described previously, the attenuation amount of the input THz power is controllable by adjusting the rotatable wire-grid

polarizer to a certain angle. The relationship of the actual power attenuation with polarizer rotation angle was calibrated with a VDI Schottky detector at both THz bands, which are not discussed in this paper. It can be clearly seen from figure 14 that, the THz HTS mixer exhibits good linearity at lower P_{THz} range. The THz power, P_{THz}, coupled into the junction was estimated from the current step-height of the Shapiro steps induced by the corresponding THz signal in the DC IVC [25] (as that shown in figure 11 but would be different step-heights according to different attenuated THz signal levels). The 1-dB compression points are at P_{THz} = -65 dBm and P_{THz} = -56 dBm for those two THz bands, respectively. Based on the P_{THz}, IF output power P_{IF} and calibrated IF link gain G_{IF}, the conversion gain G_{mix} can be estimated from $G_{mix} = P_{IF} / (P_{THz} \bullet G_{IF})$. As shown in figure 14, the G_{mix} is around -30 dB for 200 GHz band and around -50 dB for 600 GHz band. The conversion gain is comparable to that of the state-of-art semiconductor even harmonic mixer (EHM) from VDI at similar frequencies [26]. Up to the date, we are not aware any other reported conversion gain performance for HTS harmonic mixer at THz band (except for our recent reported narrow-band mixer [22]), although the observation of high-order harmonic mixing phenomenon had been reported in HTS Josephson junctions [13, 14, 16]. We attribute the good performance of the presented mixer to the excellent characteristics of our step-edge Josephson junction as well as careful electromagnetic design and analysis.

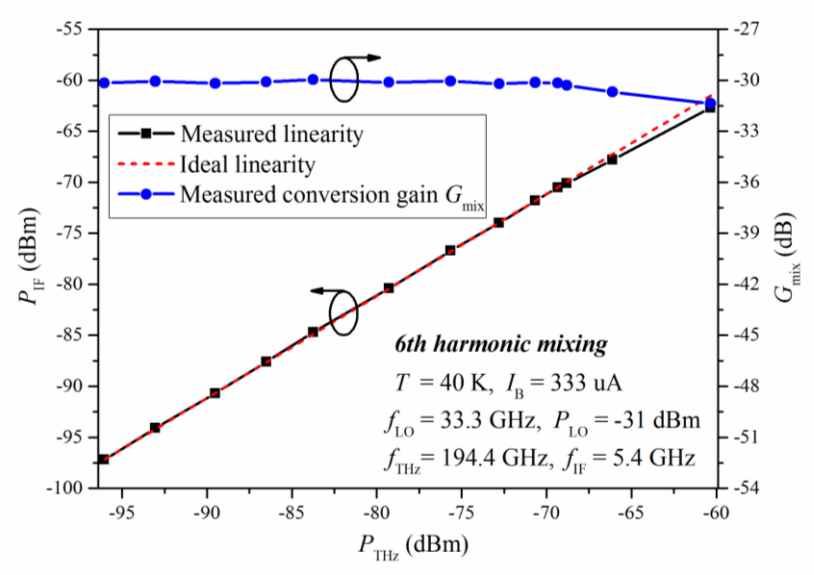

(a)

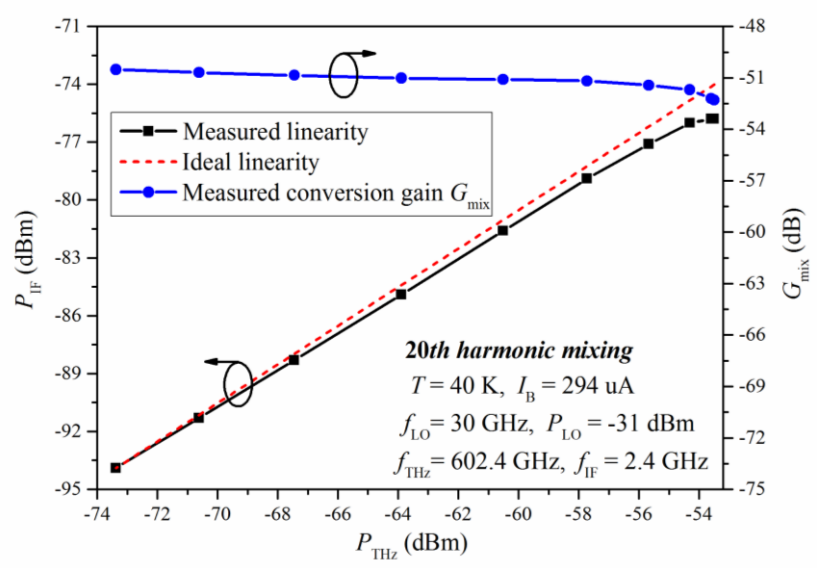

(b)

Figure 14. Linearity and conversion gain of the wideband THz HTS Josephson-junction mixer at (a) 200 GHz and (b) 600 GHz bands.

5. Conclusion

A wideband THz HTS Josephson-junction mixer was presented in this paper. The THz log-periodic thin-film antenna, microwave matching circuit as well as mixer chip package were carefully designed to improve the THz radiation coupling and microwave signal transmission. Based on the optimized design, the wideband THz HTS mixer module was fabricated and characterized to demonstrate the frequency down-conversion capability. Harmonic mixing performance was characterized at both the 200 GHz and 600 GHz bands. The mixer achieves at least 12 GHz IF bandwidth for either upper or lower sidebands, and 24 GHz instantaneous bandwidth for double-sideband operation. At bath temperature of 40 K, the measured mixer conversion gain is around -30 dB for 200 GHz band (6th harmonic mixing) and around -50 dB for 600 GHz band (20th harmonic mixing). The required LO pumping power is very low, in the order of μW. These results have demonstrated the good performance of the presented mixer and the effectiveness of our electromagnetic designs. The mixer has potential application in ultrahigh data-rate THz wireless communication systems.

Acknowledgement

The authors would like to thank our colleagues Ms Jeina Lazar for the HTS chip fabrication and Ms Mei Shen for the mixer module packaging.

References

1. Ducournau G, Szriftgiser P, Beck A, Bacquet D, Pavanello F, Peytavit E, Zaknoune M, Akalin T and Lampin J-F 2014 Ultrawide-Bandwidth Single-Channel 0.4-THz Wireless Link Combining Broadband Quasi-Optic Photomixer and Coherent Detection *IEEE Trans. THz Sci. Technol.* **4** 328-337.

2. Wang C, Lu B, Lin C, Chen Q, Miao L, Deng X and Zhang J 2014 0.34-THz wireless link based on high-order modulation for future wireless local area network applications *IEEE Trans. THz Sci. Technol.* **4** 75-85.

3. Li J, Shi S-C, Liu D, Zhou K-M, Wang M, Chen T-J, Chen C-W, Lu W-C, Chiu C and Chang H-H 2011 Noise and bandwidth of 0.5-THz twin vertically stacked SIS junctions *IEEE Trans. Appl. Supercond.* **21** 663-666.

4. Tan B-K, Yassin G, Grimes P, Leech J, Jacobs K and Groppi C 2012 A 650 GHz unilateral finline SIS mixer fed by a multiple flare-angle smooth-walled horn *IEEE Trans. THz Sci. Technol.* **2** 40-49.

5. Shan W, Takeda M, Kojima T, Uzawa Y, Shi S, Noguchi T and Wang Z 2010 Low-noise waveguide-type NbN/AlN/NbN SIS mixers approaching terahertz frequencies *IEEE Trans. Microw. Theory Tech.* **58** 841–848.

6. Irimajiri Y, Kawakami A, Morohashi I, Kumagai M, Sekine N, Nagano S, Ochiai S, Tanaka S, Hanado Y, Uzawa Y and Hosako I 2015 Development of a superconducting low-noise 3.1-THz hot electron bolometer receiver *IEEE Trans. THz Sci. Technol.* **5** 1154-1159.

7. Buchel D, Putz P, Jacobs K, Schultz M, Graf U U, Risacher C, Richter H, Ricken O, Hubers H-W, Gusten R, Honingh C E and Stutzki J 2015 4.7-THz superconducting hot electron bolometer waveguide mixer *IEEE Trans. THz Sci. Technol.* **5** 207-214.

8. Shiba S, Irimajiri Y, Yamakura T, Maezawa H, Sekine N, Hosako I and Yamamoto S 2012 3.1-THz heterodyne receiver using an NbTiN hot-electron bolometer mixer and a quantum cascade laser *IEEE Trans. THz Sci. Technol.* **2** 22-28.

9. Shimakage H, Uzawa Y, Tonouchi M and Wang Z 1997 Noise temperature measurement of YBCO Josephson mixers in millimetre and submillimeter waves *IEEE Trans. Appl. Supercond.* **7** 2595-2598.

10. Harnack O, Darula M, Scherbel J, Heinsohn J-K, Siegel M, Diehl D and Zimmermann P 1999 Optimization of a 115 GHz waveguide mixer based on an HTS Josephson junction *Supercond. Sci. Technol.* **12** 847-849.

11. Scherbel J, Darula M, Harnack O and Siegel M 2002 Noise properties of HTS Josephson mixers at 345 GHz and operating temperatures at 20 K *IEEE Trans. Appl. Supercond.* **12** 1828-1831.

12. Malnou M, Feuillet-Palma C, Ulysse C, Faini G, Febvre P, Sirena M, Olanier L, Lesueur J and Bergeal N 2014 High-Tc superconducting Josephson mixers for terahertz heterodyne detection *J. Appl. Phys.* **116** 074505.

13. Chen J, Myoren H, Nakajima K and Yamashita T 1997 Mixing at terahertz frequency band using $YBa_2Cu_3O_{7-\delta}$ bicrystal Josephson junctions *Appl. Phys. Lett.* **71** 707-709.

14. Chen J, Kobayashi E, Nakajima K, Yamashita T, Linzen S, Schmidl F and Seidel P 1999 Terahertz responses of HTS Josephson junctions on bicrystal substrates *Advances in Superconductivity XI* ed N Koshizuka et al (Japan: Springer) pp 1279-1284.

15. Harnack O, Darula M, Beuven S and Kohlstedt H 2000 Noise and conversion properties of Y-Ba-Cu-O Josephson mixers at operating temperatures above 20 K *Appl. Phys. Lett.* **76** 1764.

16. Xu W W, Zhang Y F, Jiang X K, Ling K, Chen J and Wu P H 2007 Performance improvements of a microwave oscillator using high temperature superconducting harmonic mixer *IEEE Trans. Appl. Supercond.* **17** 938.

17. Du J, Zhang T, Guo Y J and Sun X 2013 A high-temperature superconducting monolithic microwave integrated Josephson down-converter with high conversion efficiency *Appl. Phys. Lett.* **102** 212602.

18. Du J, Wang J, Zhang T, Bai D, Guo Y J and He Y 2015 Demonstration of a portable HTS MMIC microwave receiver front-end *IEEE Trans. Appl. Supercond.* **25** 1500404.

19. Zhang T, Du J, Wang J, Bai D, Guo Y J and He Y 2015 30 GHz HTS receiver front-end based on monolithic Josephson mixer *IEEE Trans. Appl. Supercond.* **25** 1400605.

20. Du J, Hellicar A D, Li L, Hanham S M, Macfarlane J C, Leslie K E, Nikolic N, Foley C P and Greene K J 2009 Terahertz imaging at 77 K *Supercond. Sci. Technol.* **22** 114001.

21. Du J, Smart K, Li L, Leslie K E, Hanham S M, Wang D H C, Foley C P, Ji F, Li X D and Zeng D Z 2015 A cryogen-free HTS Josephson junction detector for terahertz imaging *Supercond. Sci. Technol.* **28** 084001.

22. Du J, Weily A R, Gao X, Zhang T, Foley C P and Guo Y J 2017 HTS step-edge Josephson junction terahertz harmonic mixer *Supercond. Sci. Technol.* **30** 024002.

23. Balanis C A 1992 *Antenna Theory: Analysis and Design* (New York, USA: Wiley).

24. Foley C P, Mitchell E E, Lam S K H, Sankrithyan B, Wilson Y M, Tilbrook D L and Morris S J 1999 Fabrication and characterisation of YBCO single grain boundary step edge junctions *IEEE Trans. Appl. Supercond.* **9** 4281-4284.

25. Duzer T V and Turner C W 1999 *Principles of Superconductive Devices and Circuits* (Upper Saddle River, NJ, USA: Prentice-Hall).

26. Http://www.vadiodes.com.